Analyst

Accepted Manuscript

ROYAL SOCIETY OF CHEMISTRY

www.rsc.org/analyst

Monitoring Cellular Stress Responses using Integrated High-Frequency Impedance Spectroscopy and Time-Resolved ELISA

Verena Charwat[‡], Martin Joksch[†], Drago Sticker[‡], Michaela Purtscher[‡], Mario Rothbauer[‡] and Peter Ertl[‡]*

Contribution from

[‡] BioSensor Technologies, AIT Austrian Institute of Technology GmbH, Muthgasse 11, 1190 Vienna, Austria

and

[†] Corporate Technology, Siemens AG, Siemensstraße 1, Vienna, Austria

*Corresponding author:
Email: peter.ertl@ait.ac.at
Fax: +43 (0) 50550 4399

ABSTRACT

We have developed a lab-on-a-chip system for continuous and non-invasive monitoring of microfluidic cell cultures using integrated high-frequency contactless impedance spectroscopy. Electrically insulated microfabricated interdigitated electrode structures were embedded into four individually addressable microchambers to reliably and reproducibly detect cell-substrate interactions, cell viability and metabolic activity. While silicon nitride passivated sensor substrates provided a homogeneous cell culture surface that minimized cell orientation along interdigitated electrode structures, the application of high-frequency AC fields reduced the impact of the 300 nm thick passivation layer on sensor sensitivity. The additional implementation of multivariate data analysis methods such as partial least square (PLS) for high-frequency impedance spectra provided unambiguous information on intracellular pathway activation, up and down-regulation of protein synthesis as well as global cellular stress responses. A comparative cell analysis using connective tissue fibroblasts showed that high-frequency contactless impedance spectroscopy and time-resolved quantification of IL-6 secretion using ELISA provided similar results following stimulation with circulating pro-inflammatory cytokines IL-1β and TNFα. The combination of microfluidics with contactless impedance sensing and time-resolved quantification of stress factor release will provide biologist with a new tool to (a) establish a variety of uniform cell culture surfaces that feature complex biochemistries, micro- and nanopatterns; and (b) to simultaneously characterize cell responses under physiologically relevant conditions using a complementary non-invasive cell analysis method.

KEYWORDS

Microfluidics; cell chip; contactless impedance spectroscopy; multivariate data analysis; lab-on-a-chip

INTRODUCTION

In vitro cultivation of mammalian cells is an essential element of biological and medical research efforts. Since its origin over a century ago, *in vitro* cell cultures have deepened our understanding of many fundamental biological phenomena and have become an essential tool for drug development and preclinical testing.[1-3] Today the majority of approaches to analyze cell assays are based on endpoint detection methods that measure absorption, steady-state fluorescence, luminescence or radio-labeled species. Drawbacks associated with endpoint detection include a lack of dynamic information, underestimation of data artifacts and the need for complex handling steps with multiple reagents leading to low repeatability, reliability and accuracy.[3]

The recent trend towards improved, reliable and more biologically relevant assays has thus provided new opportunities for label-free technologies. An advantage of label-free cell detection methods is their ability to continuously sense cell-related changes of biophysical parameters without spatial-interference, autofluorescence or quenching effects of labels. Additionally, label-free technologies can provide information on kinetics, affinity, specificity and dose-response relationships, thus being an attractive tool for quality control and troubleshooting.[4-6] A well-established label-free analysis method is impedance spectroscopy, which provides a powerful tool for cell monitoring. The detection principle of cell impedance spectroscopy is based on the measurement of current alterations at a defined applied AC voltage which provides quantitative information on dynamic cell events including cell number variations, sensor coverage, morphological changes, cell viability, cell-to-substrate and cell-to-cell interactions.[7, 8] A variety of successful applications of cellular impedance spectroscopy have been published including cell spreading[9] and toxicity studies,[10, 11] and monitoring of cell junction formation, barrier function,[12] and stem cell differentiation.[13, 14] In recent years, the frequency-dependence of the cellular impedance signal has been increasingly used to identify specific cellular functions including micromotions,[15] cell-to-cell junction formation[16] and intracellular conductivity changes.[17] For instance, in the low frequency range (less than 1 kHz) impedance readings yield information on the extracellular microenvironment and cellular movements, while in the mid-frequency range (less than 100 kHz) predominantly membrane components and cell wall integrity are detected. However, at higher frequencies (above 500 kHz) the insulating capacity of the cell membrane can be bridged by the AC electric field and thus also allows for intracellular readings.[11]

In order to provide stable and non-drifting signals over a wide frequency range we employ contactless impedance measurements using passivated interdigitated electrode

structures (IDES).[18-20] In our previous work we have already demonstrated that complete sensor insulation physical removal from the liquid sensing environment helps to eliminate bubble formation, electrode fouling and polarization events.[21-24] Additionally, the application of a thin passivation layer allows for the establishment of a uniform sensor surface, which is important for mammalian cell cultures. It has been shown that mammalian cells are able to align along fibers and microstructures, thus influencing cell behavior.[25, 26] Therefore a passivated sensor prevents unwanted cell orientation and alignment along the electrode structures.

Despite the benefits of contactless impedance sensing a major drawback of applying insulating passivation layers on top of electrochemical sensors is associated with a loss of sensitivity. The decrease in sensor sensitivity is caused by electrical field entrapment in the respective passivation layer and is dependent on the dielectric properties and applied thickness of the passivation material. However, the influence of the insulating capacity can be theoretically reduced using high-frequency AC electric fields that are able to bridge the passivation layer. In the present research we employ impedance readings over a wide frequency range using passivated impedance sensors thereby generating large amounts of data. It has been shown that multivariate data analysis is a valid approach to extract the most relevant information from impedance spectra.[27, 28] Here we apply partial least squares (PLS) regression to reduce the data complexity and highlight relevant events in the impedance-time curves. We show that the application of a thin 300 nm silicon nitride passivation layer in combination with high-frequency AC fields and multivariate data analysis methods can be used for cell analysis.

Although impedance measurements have successfully been integrated into various microtiter plates and microfluidic assay formats, the lack of understanding of complex impedance data still limits proper interpretation of cellular phenotypic changes.[29-32] To overcome these challenges we have combined impedance spectroscopy with time-resolved ELISA of microfluidic cell cultures to generate biorelevant information on dynamic cell population responses. To combine contactless cell impedance sensing with time-resolved ELISA measurements we employed a microfluidic set up. Microfluidics allows for miniaturization, automation and integration of fluid handling and various sensory systems. Moreover, the control over cell-to-fluid volume ratios, fluid mechanical forces, continuous nutrient supply and waste removal enables the creation of stable and near physiological cell cultivation conditions. [33-38] Our novel multilevel cell-on-a-chip performs contactless impedance spectroscopy to monitor cell adhesion, cell-cell interaction and cellular activity

without disturbing normal cell behavior, while time-resolved ELISA is used to detect the release of cellular stress markers in the cell culture supernatant.

To experimentally demonstrate the practical application of our method for cell analysis, high-frequency contactless impedance spectroscopy measurements were conducted to detect (a) cell-mediated cytotoxicity activities of sub-lethal concentrations of DNA-crosslinker, (b) global inhibition of the cellular protein biosynthesis activity, and (c) the targeted activation of specific intracellular pathways. Additionally off-chip metabolic pathway detection using time-resolved ELISA was performed to help correlate the otherwise complex impedance signals to specific biological events. Figure 1a shows a conceptual overview of the applied analytical approach. Practical application of the complementary sensing approach was demonstrated by monitoring stress responses of connective tissue cells to the systemic circulating proinflammatory factors TNF-α and IL-1β. Inflammation was chosen as a relevant disease model since dynamic responses to inflammatory cytokines are associated with a variety of human disease including (microbial) infections,[39] allergies,[15] different forms of arthritis,[40, 41] cancer[42] and many others.[43]

MATERIAL AND METHODS

Lab-on-a-chip monitoring station

The high-frequency impedance measurement system shown in Figure 1b, c comprised of the microfluidic biochip sandwiched between the data acquisition board and the ceramic thermostat, a power supply and a computer-interface unit all mounted on a bench top sized board. An external syringe pump (KDS 400, KdScientific), valves (V-100D, 4-Way Valve PEEK Diagonal Flow, Upchurch) and a degasser (100 µL loop, PN7505, Postnova Analytics) were connected to the cell chip system while a lap top was used for system control and data collection. The cell chip layout consisting of a microfluidic and a sensor layer is shown in the center of Figure 1a. Microfabrication process has been described elsewhere in detail[24] and included thermal evaporation steps to deposit a 3 nm chromium as adhesion and 50 nm gold layers, photolithography using AZ MiR 701 positive photo resist (MicroChemicals GmbH) and ion milling to fabricate interdigitated electrodes (IDES) on 30 x 30 mm² glass substrates (Borofloat®, Schott). Sensor passivation was accomplished by depositing 300 nm silicon nitride (Si_3N_4) on top of impedance microelectrodes using plasma enhanced chemical vapor deposition (PECVD). The interdigitated impedance microelectrodes covered a total area of 2 mm² featuring a finger geometry of 1 mm length with 5 or 20 µm width and gap. The four microsensors were distributed at a maximum distances between adjacent measurement

circuits. Additionally, all leads were designed to feature equal length and width (100 µm) width resulting in a total resistance R = 31 Ohm, capacitance C = 1.4 pF, and inductance L = 25 nH. Cyclic voltammetry (CV) was used to assess passivation quality (300 nm Si_3N_4) by confirming complete absence of ohmic currents and faradaic contributions in the presence of 10 mM ferricyanide FCN (ferro- (60279, Fluka BioChemika) and ferricyanide (03357, Alfa Aesar)) in phosphate buffered saline (PBS; Gibco®, Life Technologies) (see suppl. information; Fig. S2a).

Microfluidic channels were formed by pouring a mixture (10:1) of PDMS (Sylgard 184) silicone elastomer base and curing agent over the epoxy master molds while polymerization was allowed to take place over a period of 4 hours at 70°C following a 10 min degassing step in a vacuum chamber. The pre-cut PDMS microfluidic was extensively cleaned using isopropanol and deionized water, activated in an oxygen plasma (Diener Electronics; (30 sec at 40 W) and put in contact with the bottom substrate under a microscope. A curing time of 24 hours at 50°C was implemented to allow complete cross-linking between the activated PDMS and Si_3N_4 surfaces.

It should be noted that the currently used version of the system has been developed as a prototype for research in a laboratory environment with expertise in cell culture, microfluidics, micro- and nanofabrication as well as statistical data analysis. However, in analogy with existing commercially available set-ups for cell impedance spectroscopy (e.g. ECIS™, Applied BioPhysics, Inc; xCELLigence, ACEA Biosciences Inc), it can easily be envisioned to advance the system into a highly automated and user friendly station that requires minimal operator training.

Mammalian cell culture handling

Normal human dermal fibroblasts (NHDF; C-12300, PromoCell) were routinely cultivated at 37°C in a 5% CO_2 humidified atmosphere as adherent monolayers in 25 cm² cell culture flasks (PAA) containing a cell density of approx. 50,000 cells/cm². DMEM high glucose medium with stable glutamine (PAA, E15-883) supplemented with 10% fetal calf serum (FCS; A15-101, PAA) was used as cultivation medium. Immortalized (telomerase) human dermal fibroblasts (HDFtert; CHT 008-0012) were purchased from EverCyte Inc. (Austria) and cultivated in medium provided by the vendor. Confluent HDFtert layers consisted of about 15,000 cells/cm². For on-chip cell cultures the media were additionally supplemented with 20 mM Hepes buffer (S11-001, PAA) and antibiotics (1% gentamicin P11-004, PAA).

Mammalian cell culture reagents

On-chip viability staining was performed using the cell-wall permeable dye calcein AM (C1430, Invitrogen). After rinsing the microreactors with PBS for 2 min, cells were exposed to 1 µM calcein AM for 5 min. Following a second rinsing step culture medium was perfused for a period of 30 min prior fluorescence imaging. Cell-surface interaction studies were conducted using the soluble adhesion factor RGDS (H-Arg-Gly-Asp-Ser-OH, 03-34-0002, Calbiochem). Aliquots of the stock solution (1.92 mM in deionized water) were stored at -20°C and added to culture medium at a final concentration of 100 or 200 µM. The pro-apoptotic substance cisplatin was purchased from Calbiochem (232120). Stock solutions of 10 mM or 33 mM in DMSO were freshly prepared before use. For inhibition of protein synthesis cycloheximide (CHX) ready solution in DMSO (C4859-1ML, 100 mg/mL, Sigma) was used. Interleukin 1-beta (IL1β) and tumor necrosis factor alpha (TNFα) were used to induce inflammatory cell responses. Human recombinant IL1β (I9401, Sigma) was applied as 10 ng/mL (from a 10 µg/mL stock in water) and TNFα (H8916, Sigma-Aldrich) was used as 25 ng/mL from 5 µg/mL stock in PBS with 0.1% human serum albumin. The selective β-adrenergic agonist isoproterenol was applied as 10 µM, purchased as hydrochloride (420355, Calbiochem) and stored as 1.2 mM stock in water.

On-chip cell cultivation

For each experiment, the microfluidic biochip was initially chemically sterilized for 30 min using 70% EtOH at 2 µL/min flow rate, followed by sequentially pumping sterile deionized water for 4h and medium for at least 2h through the microfluidic channels to remove any residual alcohol from the microchannels. Prior cell seeding the microfluidic chambers were precoated with 1 µg/mL freshly prepared fibronectin (F4759, Sigma-Aldrich®) in PBS for 20 min. Following cell harvesting from standard culture flasks, cell suspensions of the desired concentration were prepared and gently injected into the cell chips using sterile plastic syringes (1 mL). As soon as 80-100% confluence was reached, cell seeding was stopped and cells were allowed to adhere for 30 min in the absence of fluid flow. This was followed by media perfusion through activation of fluid flow to remove dead or non-adherent cells. Flow rates were adjusted to 4 µL/min to ensure continuous medium exchange. Cell attachment, movement and spreading as well as viability were monitored using in-house built electronics and data acquisition system.

High-frequency impedance sensing using contactless dielectric microsensors

The in-house designed hardware enabled impedance recording over a large frequency range (500 Hz to 20 MHz) and was based on an asymmetric controlled bridge. The data acquisition board was designed to have operational amplifier located in close proximity to the

actual impedance microsensors to allow for low noise measurements at high frequencies. Hardware components were designed to detect capacitance changes in the range of 1 pF to 10 nF with a resolution of 0.1%. The customized measurement software was developed by Siemens AG and allowed for the adjustment of a variety of impedance measurement settings including frequency range, step size with logarithmic or linear spacing of the frequencies, idle time between measurements, gain for signal amplification and several options for averaging of impedance readings. The software also contained a standard algorithm for noise reduction. During cell culture experiments, for each of the four individually addressable IDES sensor impedance and phase shift values at different frequencies (50 kHz to 5 MHz) were sequentially recorded over time (measurement cycle was less 2 min for all four sensors recording ca. 150,000 impedance data points over 24h).

Multivariate data analysis of impedance spectra

To assess the generated large impedance data sets multivariate data analysis methods were applied to analyze the time-resolved impedance spectra. The PLS package R (R Project for Statistical Computing),[44] was used to perform partial least squares (PLS) regression on impedance-time data. PLS regression is an extension of multiple linear regression that is particularly suited for problems with many, possibly correlated, predictor variables and few observations. This characteristic makes PLS an interesting tool for many applications in natural sciences. For instance PLS approaches have been successfully employed for analysis of near-infrared (NIR) spectra[45, 46], molecular activity prediction from molecular structures[47], tumor classification[48], analysis of high-dimensional genomic data[49, 50] and biological image analysis[51, 52]. Partial least squares regression is based on principal component analysis of both the input matrix (impedance spectra) and the response matrix (output values of the model) to identify the most important parameters out of both data matrices. In PLS regression, the model parameters are chosen so that the sum of squared distances between data and prediction values are minimized. Supplementary Figure S1 outlines the concept of PLS regression performed on spectral impedance data. For our experimental data the resulting model was evaluated using a training data set which consisted of cycles with known cell events. The one-step PLS model for cell culture monitoring was based on one value per spectrum, indicating whether cells are present (value near 1) or not (value near 0), which defines either "confluent

cell layer" (value 1) or "no cells" (value 0). The employed multi-step model consisted of values 0, 1, 2 that related to "no cells", "confluent cell layer2 and "stressed cell layer" to identify cellular responses to external stimuli, respectively. The optimized number of principle components for each experiment was determined by root mean square error of prediction (RMSEP) based on cross validation using leave-one-out algorithm.

Cell cycle analysis and viability using flow cytometry (FACS)

BD FACSCanto II analyzer (equipped with blue, red and violet lasers) with BD FACSDiva data acquisition software was used to assess cell cycle arrest and viability. Unless stated otherwise 10,000 events were counted for each sample. LIVE/DEAD® viability/cytotoxicity kit for mammalian cells including calcein AM and ethidium homodimer-1 (MP 03224, Molecular Probes – Invitrogen™) was used for cisplatin toxicity testing according to manufacturer's instructions. Cells were seeded to confluence in 12 well plates and cultivated for 24 h before increasing cisplatin concentrations up to 1 mM were added (total DMSO content was 3% in each well) to the cell culture medium. After 24 h incubation cells were harvested, stained and analyzed. All samples were run in triplicates. Flow cytometric cell cycle analysis method was used to quantify cells in gap 0 / gap 1 (G0/G1), synthesis (S) and gap 2 / mitosis (G2/M) phase. For cell cycle analysis cells were harvested and fixed with 2% paraformaldehyde for 10 min. Then cells were permeabilized using 0.2% triton X 100 (H5142, Promega), resuspended in PBS with 0.2% bovine serum albumin, stained with 5 µg/ mL DAPI (4′,6-diamidin-2-phenylindol, D1306, Invitrogen) from a 5 mg/ mL stock in water and analyzed. Histograms of blue fluorescence intensity showed a G0/G1 peak (2N) and a G2/M peak (4N) with a 2x higher fluorescence. S-phase cells appeared between the two peaks. G0/G1 population was calculated as twice the cell number between center of peak 1 and its left shoulder. G2/M population was calculated as twice the cell number between center of peak 2 and its right shoulder. The remaining cells were declared as S phase population (100% minus percent in G0/G1minus percent in G2/M).

Biochemical screening for cytokine release using time-resolved ELISA

For quantification of the inflammation marker interleukin-6 (IL-6) an ELISA kit for human IL-6 (READY-SET-GO #88-7066-88, eBioscience) was used according to the manufacturer's instructions. Aliquots of 20 µL supernatant from the cell cultivation chambers were subsequently collected and stored at -80°C until analysis. For colorimetric read-out an infinite 200 plate reader (Tecan AG) with Tecan i-control software (V 1.6.19.2) and 450 nm absorbance filter was used (4 readings/well). Samples were analyzed in duplicates and whenever necessary, pre-diluted (2 to 10-fold) to be within the defined concentration range.

RESULTS AND DISCUSSION

Characterization of the lab-on-a-chip system for high-frequency impedance cell analysis

One aim of this research was the development and characterization of a hybrid cell chip technology capable of continuously monitoring dynamic mammalian cell population responses to systemic circulating inflammation markers using contactless high-frequency impedance spectroscopy. To provide a uniform cell culture substrate that minimizes cell orientation along the interdigitated electrode structures (Figure 2a i), impedance biosensors were covered with a 300 nm Si_3N_4 layer. Figure 2a shows microscope images of microfluidic NHDF cultures on microelectrodes taken after 6 hours (including seeding, attachment and spreading) in (i) the absence and (ii) presence of an insulation layer. Complete sensor insulation was confirmed using CV in the presence of the electroactive compound FCN (see suppl. information; Fig. S2a). Additional characterization was performed by measuring frequency-spectra of the open system (without chip), passivated IDES with deionized water and three isotonic solutions including PBS, medium and medium supplemented with 10% fetal bovine serum (see suppl. information; Fig. S2b and c). Impedance signals of cell culture medium revealed excellent signal stability during several days of operation and exhibited less than <0.1% noise contribution to the base line impedance-time trace - typically between 0.01% at high frequencies (above 1 MHz) and 0.04% at lower frequencies (100 kHz) (data not shown). To evaluate frequency-dependency of contactless cell impedance sensing, anchorage-dependent human cell cultures were initially assessed using two IDES sensor geometries (finger width and gap of 5 µm or 20 µm). Results of the frequency analysis are shown in Figure 2b where relative impedance differences (n=4) in the absence and presence of human dermal fibroblasts are plotted over the entire frequency range (10 kHz to 20 MHz). Although both the 5 µm and 20 µm microsensors exhibited highest signal changes between 1 MHz to 5 MHz the larger IDES geometry revealed better performance over the entire frequency range that point at an improved electrical field distribution within the confluent cell monolayer. Additionally, calculated signal-to-noise ratios (|Z|_cell-|Z|_medium/ 3xStDev (|Z|_medium); n=7) listed in Table 1 showed higher sensitivity in the higher frequency range in the presence of the larger (20 µm) impedance sensor design. In an attempt to facilitate physical interpretation of the measured impedance spectra an electrical equivalent circuit was established using complex non-linear least square fitting with a freeware program (EIS Spectrum Analyser 1.0). Initial computational results using PBS impedance spectra confirmed that the chosen electric circuit diagram (see suppl. Information; Fig. S3), which

also accounts for gold leads, the passivation layer and the electrolyte concentration, can be used to estimate resistive and capacitive contributions to the high-frequency impedance signal. For instance, at the present configuration the resistive part of the impedance involving electrolyte contributions dominates above 2 MHz where phase values shifted towards zero (0) degrees, thus indicating that the influence of the passivation layer can largely be neglected above the critical frequency (2 MHz).

Next, sensor to sensor variations within a single microchip were investigated during the formation of confluent fibroblast cell layer over a period of 16 h in the four adjacent cell culture chambers. While similar impedance set-off values were found between neighboring sensors (sensor positioning is shown in the inset of Figure 1c), the more distantly located impedance sensors displayed set-off values of 611 Ohm and 664 Ohm (at 5 MHz) that point at fabrication inconsistences in the passivation thickness across the biochip. Despite the difficulty of introducing identical cell numbers in each microchamber, comparable adhesion curves were obtained (at 5 MHz) for all four microsensors (see Figure 3a). Additional evaluation of the contactless high-frequency cell impedance chip system included cell-substrate interaction and cytotoxicity measurements in subsequent experiments. Figure 3b shows high-frequency impedance measurements of NHDF cell cultures that were also challenged with the soluble integrin binding peptide RGDS (red lines). RGDS is a soluble peptide that contains the integrin binding sequence RGD (ARG-GLY-ASP) and plays an important role *in vivo* as an extra cellular matrix motif that controls cell-matrix interaction. RGDS was applied at two concentrations 100 and 200 µM and resulted in a marginal impedance increase of less than 5 Ohms, indicating reduced cell attachment resulting in minimal sensor coverage. Additionally, two different cell densities (100% and 50% confluence or 25,000 cells/cm^2) were employed to assess the effect of sensor coverage on impedance signals as seen in Figure 3b (black traces). While microscope images (see also suppl. information; Fig. S4) confirmed the inability of NHDF cells to attach to the microreactor surface during exposure of the cell adhesion blockers, the 50% reduction of cell number resulted in an impedance decrease from 30 Ohm to 15 Ohms. The observed impedance decrease confirmed the ability of the contactless biosensor to detect variations of cell surface coverage within the microreactors. Furthermore, cell recovery experiments shown in Figure 3c revealed a rapid impedance signal increase within the first 6 h following the removal of RGDS from the cell culture medium. However the obtained significantly lower impedance plateau after 8 h points at a reduced surface coverage pointing at a reduced cell viability and inability to fully attach to the microchip surface. Overall, the experiments

confirmed high sensitivity of the sensor system towards changes in surface coverage. In the case of 200 µM RGDS image analysis showed that 10 to 15% of the sensor area was covered with cells yielding a small but still detectable signal increase of 2.5 to 5 Ohms at 5 MHz. These results are in line with cell sensitivity found in a similar setups[53] and indicate a detection limit of about 5,000 cells/ cm² or 100 cells located above the IDES.

Final biosensor characterization involved the application of the cytostatic agent cisplatin known to trigger programmed cell death by crosslinking DNA to also confirm the ability to detect cell damage and apoptosis. Standard viability/ cytotoxicity assays were first employed to determine dose-response relationship using flow cytometry (see suppl. information; Fig. S5a) resulting in a dose (LD_{50}) of 300 µM where approx. 50% of the fibroblast cell population died after 24 h exposure to cisplatin and a minimum inhibitory concentration (MIC) of approx. 50 µM. The addition of 300 µM cisplatin at two different time points (12 h and 25 h) to the microfluidic cell culture showed reproducible impedance decreases of -1.3 ± 0.3 mOhm/min (see Figure 4a), while control measurements using cell-free medium exhibited no significant impedance differences in the absence and presence of 1 mM cisplatin (data not shown). However, cellular responses to MIC level concentration of cisplatin (80% viability after 24 h) could not be detected by the high-frequency impedance analyzer. Normalized impedance curves of NHDF cell cultures of which two cell chambers were treated with 50 µM cisplatin over a 16 h culture period showed no clear signal changes in response to the drug (impedance data at 5 MHz is shown in Figure 4b and 120 kHz suppl. information; Fig. S5b). Also visual inspection did not reveal any morphological differences between treated and untreated cells (images not shown).

Multivariate data analysis of high-frequency impedance spectra

In an attempt to further improve sensitivity of the developed cell chip system, multivariate data analysis of time-resolved impedance spectra was employed to help clarify ambiguous single frequency data. Frequency analysis in Figure 2b already indicated that cellular information is contained using frequencies ranging from 100 kHz to 10 MHz. Partial least squares regression (PLS) was selected as analysis method, because it is known to eliminate irrelevant signal variations such as noise, drift and artifacts thus emphasizing on biological factors that cause impedance changes. The PLS method was initially validated using a number of impedance spectra obtained in the absence and presence of NHDF cell adhesion measurements (data not shown) and then employed to analyze indefinable impedance measurements. As an example, Figure 5a shows PLS analysis of NHDF cultures treated with sub-lethal concentration of cisplatin. Results of the multivariate impedance data

analysis indicate that the employed PLS method allows for discriminating between MIC level concentration of cisplatin (50 µM) treated and control measurements. Also, cell population responses to a non-toxic concentration of cycloheximide (CHX) were investigated in subsequent experiments to better highlight the benefits of using the PLS analysis method. CHX is a well-known bacterially derived inhibitor of eukaryotic protein synthesis that interferes with translational protein elongation by blocking translocation of tRNA and mRNA at the ribosome. CHX is typically applied in working concentrations between 1 and 100 µg/ ml to inhibit >90% of protein biosynthesis.[54] Figure 5b shows PLS analysis of impedance-time traces (impedance data at 5 MHz is show in suppl. Information; Fig S6a) of two NHDF cell cultures that were repeatedly challenged over a period of 6 days with CHX. The alternating exposure to a low CHX concentration of 1 µg/ ml (starting after 48 h) yielded reproducible and reliable cell responses during three consecutive 12 h treatment and 12 h recovery periods. Control measurements of cell-free and untreated samples (see suppl. information; Fig. S6b and S6c) did not show any significant signal changes. Visual inspection of the cell cultures revealed no discernible morphological differences between normal and CHX treated cells. To further demonstrate the ability of contactless high-frequency impedance spectroscopy to also detect defined intracellular events, dynamic cell responses to a target specific stimulant was investigated in subsequent experiments. Isoproterenol was chosen as a single receptor target model because it is known to selectively stimulate β-adrenergic receptors of intracellular adenyl cyclase, thus effectively activating the conversion of adenosine triphosphate (ATP) to cyclic- 3',5'- adenosine monophosphate (c-AMP).[55, 56] Although impedance raw data could readily identify NHDF cells culture responses following alternating isoproterenol treatments, additional PLS analysis shown in Figure 5c further emphasized the dynamic cellular responses.

Encouraged by the above results the serum component (FCS) of the cell culture medium was removed in subsequent experiments to analyze starvation responses from healthy cell cultures. A limited nutrient supply results in a lowered protein biosynthesis and decreased cellular activity that cannot be readily identified by microscopic observation and therefore requires more complex cell analysis methods such as FACS, ELISA and others. In a first set of experiments, high-frequency impedance spectroscopy and PLS data analysis was used to assess dynamic cellular starvation responses, while time-resolved ELISA was conducted to verify changes in cellular metabolism. Since inflammation responses such as the release of cytokines by human synovial, dermal, lung and other tissue fibroblast play a key role in their natural function, quantitation of IL-6 production was chosen as an indicator of cellular

activity. PLS analysis of impedance-time traces showed a rapid signal decrease during the 12 h serum starvation period that is followed by a recovery after the addition of 10 % FCS (see Figure 6a). Concurrently, corresponding time-resolved ELISA of fibroblast cell culture supernatant revealed complete elimination of cellular IL-6 production and release within a 12 h serum-starvation period (see Figure 6b). Since additional flow cytometry analysis showed no induction of cell cycle arrest by serum starvation over period of 48 h (see suppl. information; Fig. S7a), these results indicate down and up-regulation of IL-6 biosynthesis. Table 2 lists additional flow cytometry results of NHDF cell cultures that have been starved for a period of 0 to 72 h prior addition of 10 % serum containing medium for subsequent 26 h. Only extended starvation periods (>48 h) revealed a significant increase in cell numbers in the G2/M phase. These results demonstrated that a 12 h serum-starvation did not lead to a detectable cell cycle arrest thus confirming the decreased interleukin biosynthesis activity as indicated by the time-resolved ELISA. To further investigate dynamic cellular responses to serum starvation, high-frequency impedance spectroscopy following repeated and alternating removal of 10% FCS was conducted (see also suppl. information; Fig. S7b). PLS-analysis during repeated serum-starvations is shown in Figure 6c where the application of serum-free medium was alternated every 12 h. It is important to note that only the time-dependent signal change carries biological information, while the direction of signal change solely depends on the employed computational PLS model. The similar and reproducible trend which can be clearly seen between the four microfluidic cell cultures also correlated well with the on- and off switching of the IL-6 synthesis machinery as shown by the time-resolved ELISA (Figure 6d).

Monitoring cellular stress responses to systemic proinflammatory factors

Next, practical application was demonstrated by monitoring global stress responses of connective tissue cells to systemic circulating proinflammatory factors. It is well known, that inflammation responses of *in vitro* cell cultures can be artificially induced by a variety of pro-inflammatory cytokines such as interleukin IL-1 β and tumor necrosis factor alpha (TNFα). The main response of fibroblasts to inflammatory stimuli includes remodeling of the extra cellular matrix (ECM). The underlying mechanisms involve up-regulation of matrix metalloproteinases (MMPs), which degrade various ECM compounds, as well as reduced expression of the ECM compounds collagen and fibronectin.[57, 58] These tissue remodeling processes result in significant cell population changes including variations in cell morphology, altered cell-substrate interaction and changes in cell-to-surface distance that are detectable by impedance spectroscopy. This means that impedance measurements

simultaneously detect a broad range of cellular responses and do not provide specific information on the underlying biological origin of a signal change. Since IL-6 is a well-known biomarker for inflammatory cell responses of fibroblast cultures, we performed time-resolve ELISA tests to link impedance data to IL-6 expression. In a final set of experiments cellular stress responses of normal (NHDF) and immortalized (HDFtert) fibroblast cell cultures were investigated following stimulation using the proinflammatory cytokines IL-1β and TNFα. The applied concentrations of 10 ng/ ml for IL-1β and 25 ng/ ml for TNFα were chosen as typical concentrations found in literature for induction of inflammatory cell responses in fibroblast cultures.[59-61] Figure 7a shows PLS analysis of cellular stress responses of fibroblasts (HDFtert) that were treated with 10 ng/ mL IL-1β for a period of 12 h during a 24 h culture period. Results of the study demonstrated that PLS is able to clearly identify differences in the impedance spectra between the control measurement and the IL-1β exposed fibroblast cell culture. In a next set of experiments repeated cell responses and recovery kinetics following sequential IL-1β stimulations was investigated using four confluent NHDF cell cultures. Prior to the application of alternating IL-1β exposures setup, the four NHDF cell cultures were preincubated with low-serum (2 % FBS) containing medium for a period of 24 h to decrease baseline IL-6 production (see also Figure 6b). PLS analysis shown in the upper panel of Figure 7b revealed a reproducible signal pattern that correlated well with detected IL-6 release using time-resolved ELISA (lower panel of Fig. 7b). Results of this study showed that increasing and decreasing IL-6 secretion by fibroblasts matched obtained PLS analysis, thus demonstrating for the first time that transient biological responses can be readily identified using a label-free and non-invasive analysis method. In a similar set of experiments immortalized fibroblasts were exposed to TNFα to demonstrate the ability of the high-frequency impedance cell chip to detect global stress responses to systemic and circulating proinflammatory factors. Figure 7c shows PLS analysis control and 25 ng/ mL TNFα treated cell cultures. Despite the obtained signal variations a clear difference between stimulated and non-stimulated cell cultures were found. Additional time-resolved ELISA quantitation of IL-6 secretion shown in Figure 7d confirmed that HDFtert fibroblasts can be stimulated in the presence of IL-1β and TNFα. These results demonstrate that our complementary cell analysis method can be used to monitor the complex and dynamic responses of connective tissue cells with systemic and circulating proinflammatory factors.

CONCLUSION

We have developed a complimentary non-invasive cell analysis method to assess the transient cell responses of connective tissue cells following stimulation with circulating proinflammatory responses using high-frequency contactless spectroscopy in combination with time-resolved ELISA. A key-feature of the biochip was the deposition of a 300 nm silicon nitride passivation layer on top of the electrodes (a) to support efficient PDMS bonding and reliable fabrication of hybrid biochips; (b) to prevent charge transfer which could lead to protein denaturation (c) to improve PDMS-microfluidics to sensor substrate bonding specifically along the gold leads; (d) to provide a uniform cell culture surface that can easily be modified with cell adhesion peptides using standard linker chemistries; and (e) to minimize cell orientation along interdigitated electrode structures, which we have also occasionally observed in our cell chip systems. To compensate for the loss of sensitivity using passivated electrodes, high-frequency AC fields were applied to bridge the insulation capacity. Computational analysis suggested that above a critical frequency the influence of the passivation layer can be neglected, thus resulting in highest sensor sensitivity for cell analysis.[62] Performance evaluation of our cell chip system showed long term stability, good reproducibility and adequate sensitivity and selectivity towards cellular structures. To achieve a higher sensitivity towards lower cell numbers or even single-cell resolution, a different electrode design is required as shown by several publications that have demonstrated the feasibility of impedance spectroscopy for single-cell analysis.[63, 64]

Our results further indicate that the application of multivariate data analysis methods is particular useful in highlighting dynamic cell behavior. The combination of microfluidics with time-resolved analysis of biomarker release further allowed the correlation between observed impedance changes with biological responses, thus providing biorelevant information on health status of the cell culture. Altogether, cell cycle analysis using flow cytometry, quantitation of cytokine production and release using time-resolved ELISA and microscopy suggest that contactless impedance sensors allow the reliable detection of rapid cell kinetics and intracellular activities with good time resolution and selectivity.

ACKNOWLEDGEMENT

The authors thank the Austrian Research Promotion Agency (FFG supported project #824885) for financial assistance.

FIGURE LEGENDS

Figure 1: (A) Schematic drawing of the microfluidic biochip consisting of four individually addressable cell cultivation chambers and step-by-step cell analysis: Step 1 includes the generation of time-impedance data using passivated (300 nm Si_3N_4) microimpedance sensors (IDES) that lead to 3D impedance spectra. Step 2 involves statistical data analysis and data reduction using partial least squares (PLS) analysis (data of 8 h serum starvation (no FCS) shown). Step 3 and 4 includes biochemical screening for cytokine secretion in the cell culture supernatant using time-resolved ELISA and exposure to additional cellular stress factors. (B) Benchtop-sized high-frequency impedance cell monitoring platform consisting of the microchip located in an electrical ceramic heater, measurement board and laptop. (C) Picture of the in-house built measurement board to perform impedance spectroscopy over a frequency range from 10 kHz to 20 MHz. The inset shows the microfabricated cell chip with four individual cell chambers and impedance sensors.

Figure 2: (A) Bright field images of NHDF cells cultivated for 6h on gold IDES (5 µm geometry; 50 nm height) either without (i) or with (ii) a 300 nm Si_3N_4 passivation layer. Scale bars represent 400µm. (B) compares sensitivity of two different sensor geometries (5 µm (red) and 20 µm (black)) towards cell adhesion over a range of frequencies. The relative change of |Z| between cell-free and fully cell-covered sensors was calculated from 4 individual sensors.

Figure 3: (A) Time-impedance traces (at 5 MHz) of cell seeding (at 2h), adhesion and formation of cell layers in 4 microreactors. Impedance differences (Δ|Z|) are calculated for each microsensor between cell-free and fully covered sensor surface. (B) NHDF cells were seeded at time point 0 in the absence (black lines; control) or presence of 100 or 200 µM of the soluble integrin binding peptide RGDS (red lines). In addition to NHDF cells forming a confluent layer (100%), also half the cells (50%) were seeded to demonstrate the impact of cell numbers on impedance adhesion curves. (C) NHDF cells were seeded with a 100 µM RGDS containing medium (red) or a control culture medium (black). After 84 min (arrows), the culture medium was replaced with RGDS-free medium in both cases. A partial recovery of RGDS-pretreated cells was monitored.

Figure 4: (A) Normalized impedance-time traces (5 MHz) of NHDF cultures following exposure to 300 µM (LD_{50}) cisplatin added after 12 h (red) and 25 h (black) as indicated by arrows. (B) Normalized impedance-time traces of three confluent NHDF cultures in the absence (black) and presence (red) of 50 µM cisplatin (arrow). Curves are normalized to impedance values prior cisplatin exposure.

Figure 5: (A) PLS analysis of the 50 µM cisplatin treated NHDF cell cultures. Arrow indicates addition of cisplatin. (B) PLS analysis of NHDF cell cultures exposed to repeated 1 µg/mL cycloheximide treatment of 12 h. Bars indicated perfusion with cycloheximide containing (CHX) or control medium (C) PLS analysis of target specific cell responses to repeated exposure to 10 µM isoproterenol.

Figure 6: (A) PLS analysis of fibroblast cell culture response (arrow indicates cell seeding) following 12 h serum starvation. (B) Quantification of interleukin 6 (IL-6) release measured in aliquots of supernatant collected from microfluidic NHDF cultivation using time-resolved ELISA. (C) PLS analysis of repeated and alternating serum starvation (no FBS) of four NHDF cell chambers induced after 30 h in culture. Serum starvation was started in the chambers indicated in red (a) and after 12 h switched to chambers indicated in black (b). Then the pattern was repeated. The vertical line indicates medium changes at 59 h for all chambers. (D) ELISA quantification of IL-6 in supernatants collected from microfluidic cell culture shown in C). The red and black lines match with the respectively colored samples in C).

Figure 7: (A) PLS analysis of impedance spectra following 10 ng/mL IL-1β (red) treatment of microfluidic HDFtert fibroblast cell cultures. (B) PLS and time-resolved ELISA measurements of 24 h with 2% FBS pre-treated NHDF cells that have been alternatingly exposed to 10 ng/mL IL-1β (periods are indicated by black and red bars) between different chambers. Lower panel shows time-resolved ELISA quantification of IL-6 secretion during IL-1β exposures. (C) PLS analysis of impedance spectra using HDFtert fibroblasts cultivated in a flow chamber and exposed to 25 ng/mL TNFα. (D) Time-resolved ELISA quantification of IL-6 secretion during TNFα exposure.

Table 1: Impedance changes of a confluent cell layer compared to background noise from n = 4 sensors for two different IDES geometries.

selected frequency *f*	Signal to noise ratio (S/N) of two IDES sensors 5x5 µm	20x20 µm
158 kHz	5.1 ± 3.1	35.6 ± 3.9
316 kHz	8.7 ± 1.3	44.5 ± 5.3
631 kHz	12.5 ± 3.0	53.9 ± 3.1
1.26 MHz	16.6 ± 7.5	55.9 ± 7.3
2.51 MHz	20.2 ± 6.4	67.4 ± 18.0
5 MHz	16.3 ± 2.9	48 ± 18
10 MHz	8.4 ± 2.7	35.1 ± 10.7

* Averaged impedance values of four repetitive measurements

Table 2: Cell cycle distribution of NHDF serum starved NHDF cell cultures as mean cell count ± standard deviation.

Starvation time (+26 h 10% FBS)	cell population [%] G0/G1	S	G2/M
0 h	57.8 ± 4.7	13.7 ± 2.3	28.5 ± 4.5
6 h	55.3 ± 0.7	13.6 ± 4.7	31.0 ± 4.8
12 h	58.6 ± 2.1	11.9 ± 2.7	29.4 ± 1.8
24 h	53.9 ± 5.6	10.6 ± 4.3	35.5 ± 9.5
48 h	48.9 ± 0.9	10.0 ± 2.2	41.1 ± 1.7
72 h	38.9 ± 2.1	11.4 ± 1.4	49.7 ± 3.5

* Averaged values of 6 repetitive measurements

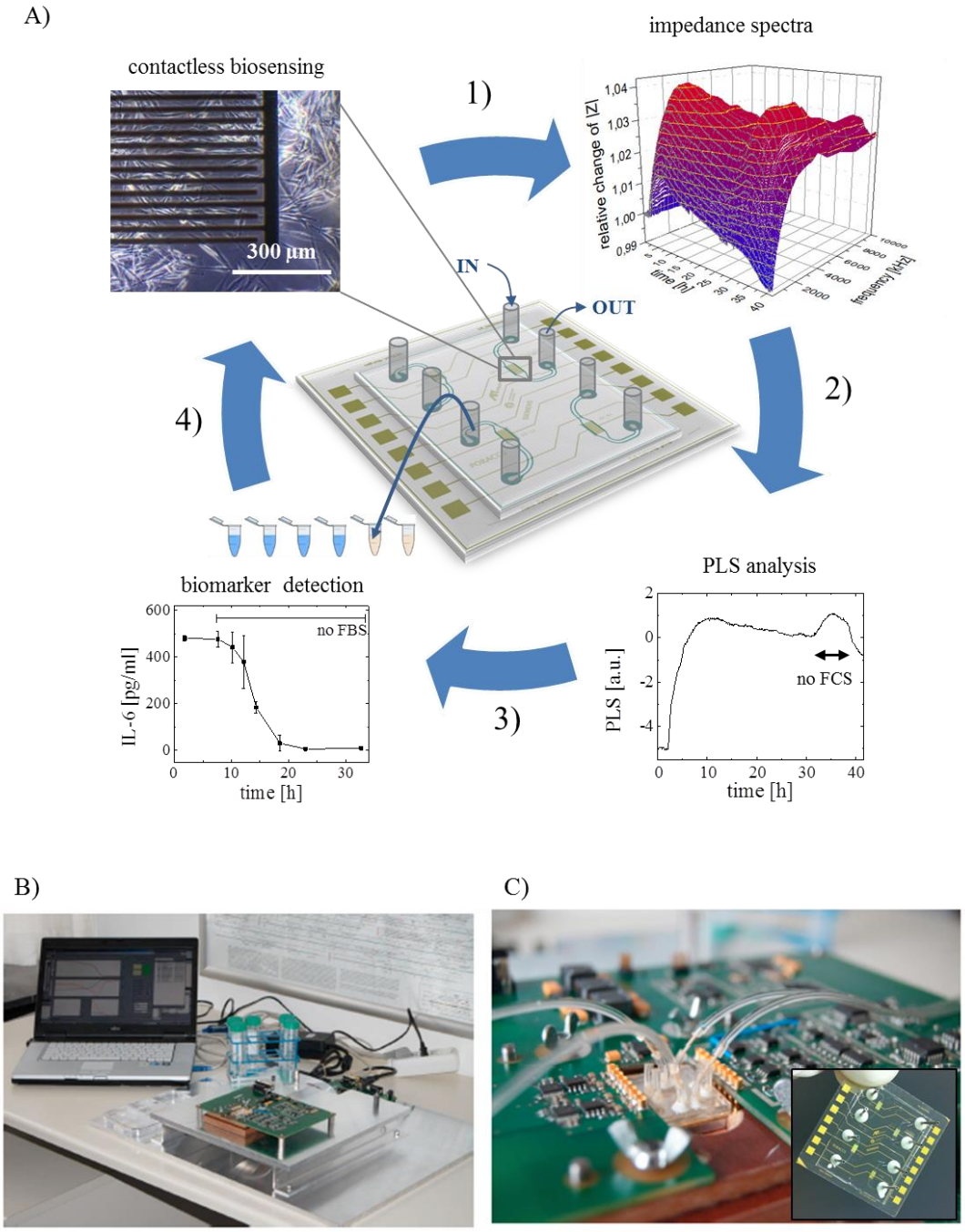

Figure 1

A)

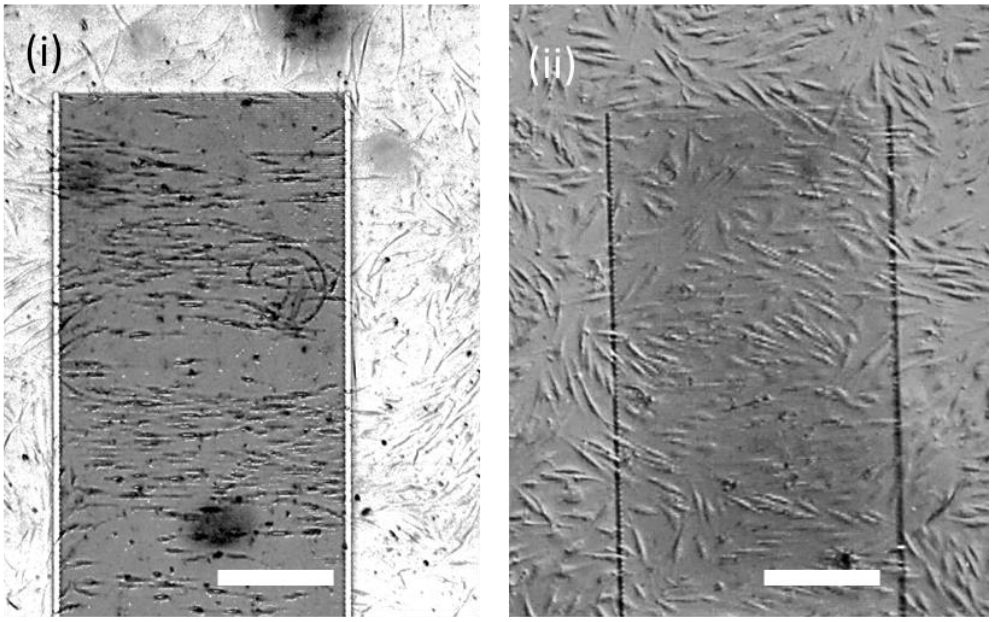

B)

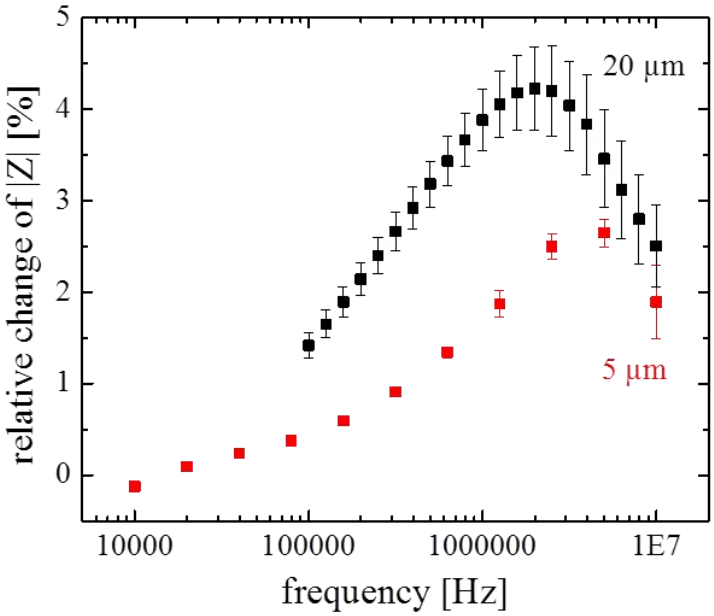

Figure 2

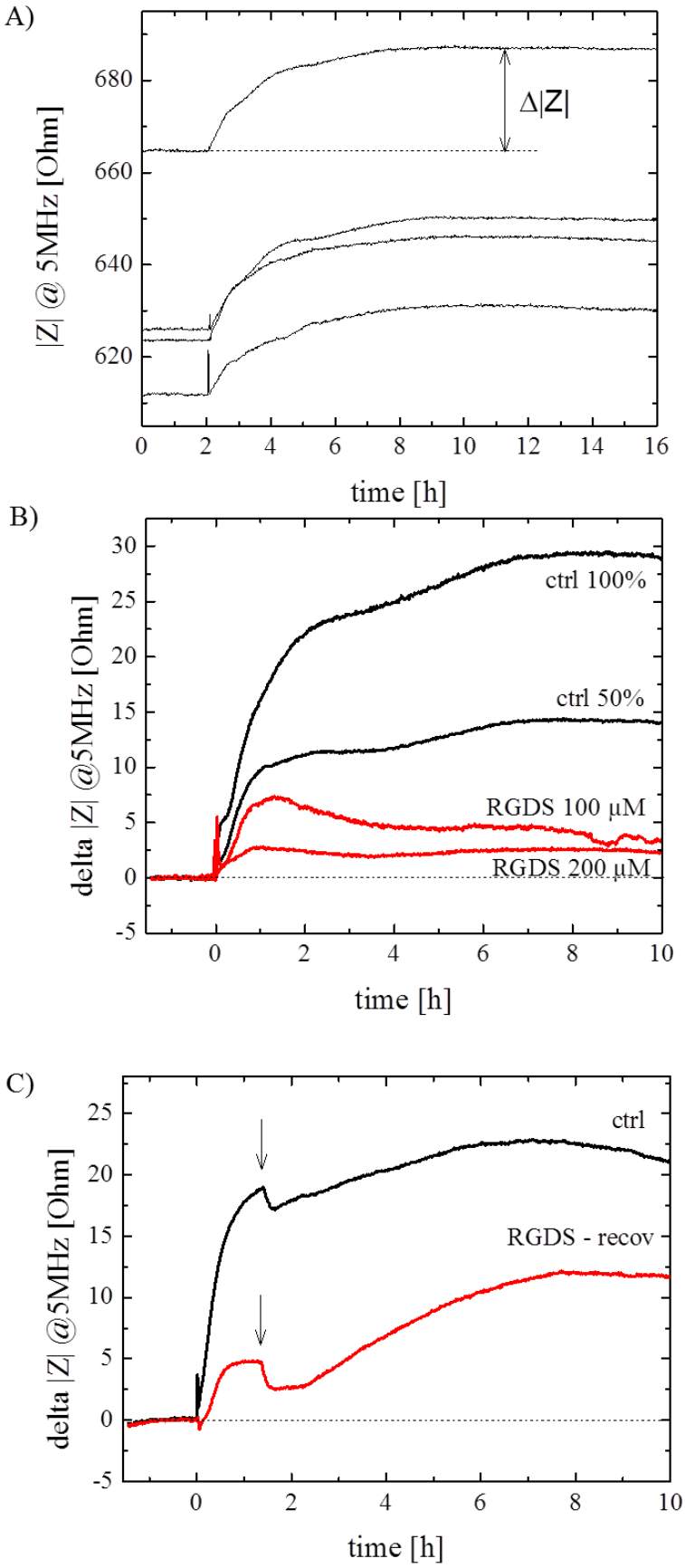

Figure 3

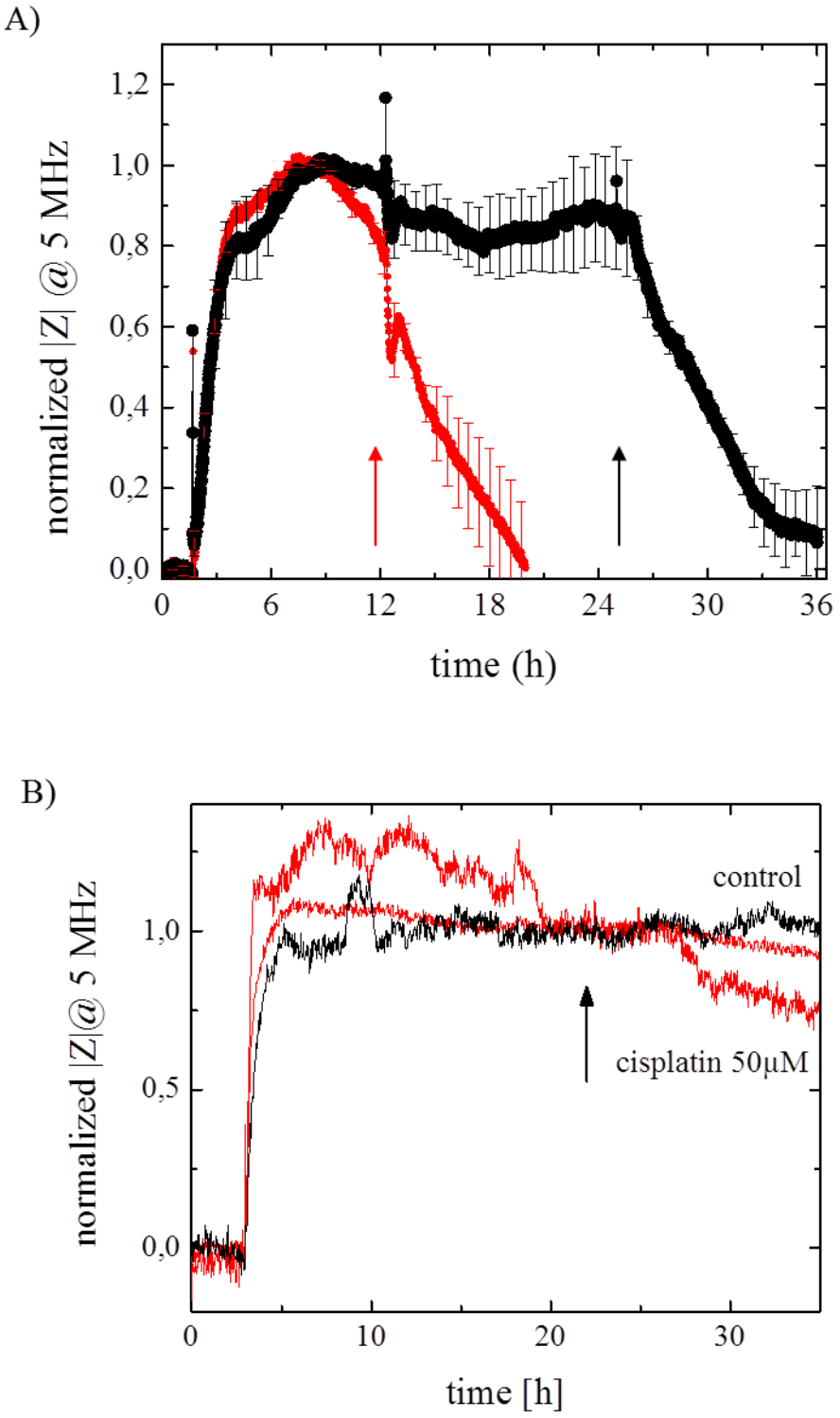

Figure 4

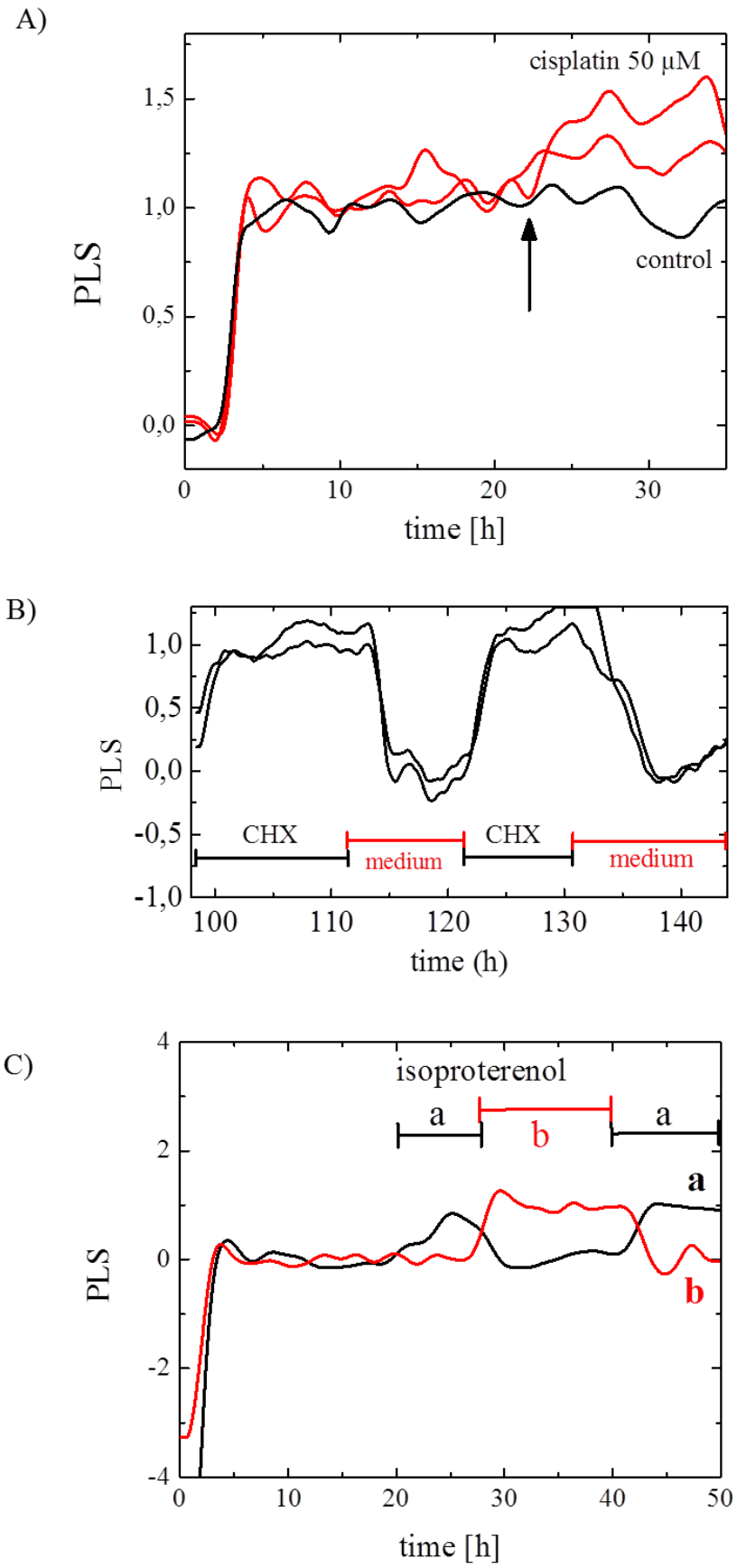

Figure 5

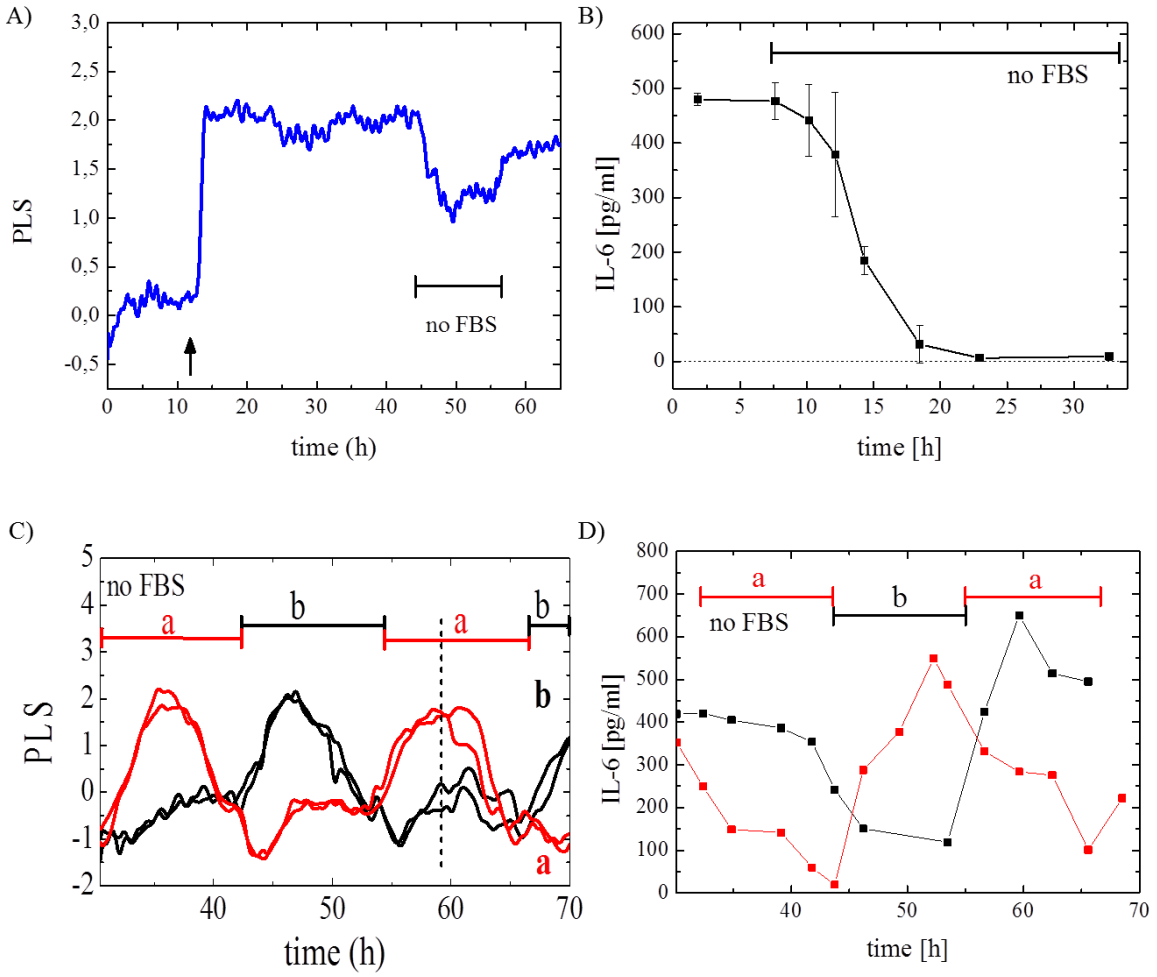

Figure 6

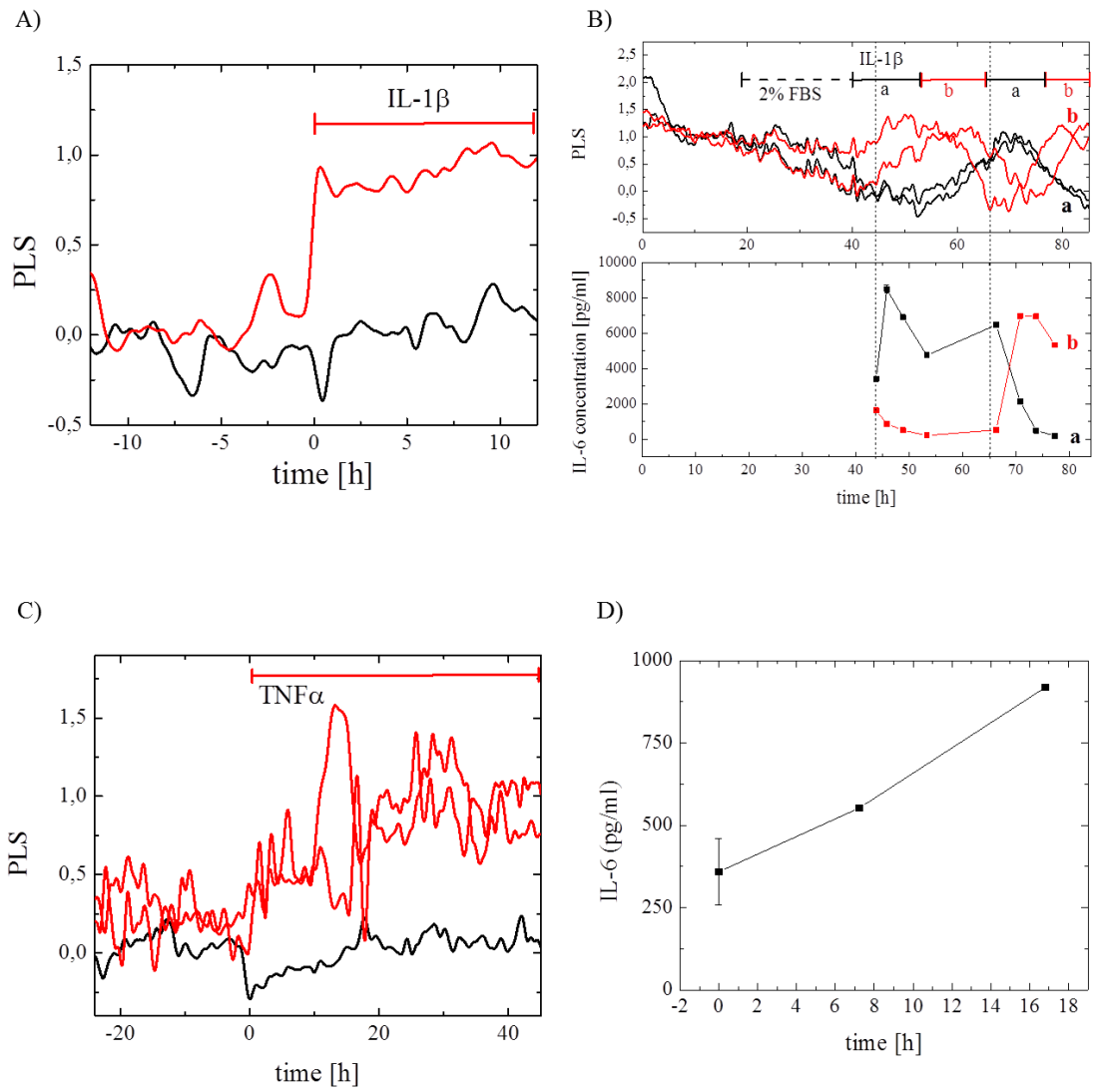

Figure 7

REFERENCES

1. W. F. An and N. Tolliday, *Mol Biotech*, 2010, **45**, 180-186.
2. J. Drews, *Science*, 2000, **287**, 1960-1964.
3. E. Michelini, L. Cevenini, L. Mezzanotte, A. Coppa and A. Roda, *Anal Bioanal Chem*, 2010, **398**, 227-238.
4. M. A. Cooper and L. Mayr, *Label-free technologies for drug discovery*, Wiley Online Library, 2011.
5. S. M. Shamah and B. T. Cunningham, *Analyst*, 2011, **136**, 1090-1102.
6. A. Pierzchalski, M. Hebeisen, A. Mittag, J. Bocsi, M. Di Berardino and A. Tarnok, *Lab Chip*, 2012, **12**, 4533-4543.
7. M. E. Orazem and B. Tribollet, *Electrochemical impedance spectroscopy*, Wiley-Interscience, 2011.
8. V. F. Lvovich, *Impedance spectroscopy: applications to electrochemical and dielectric phenomena*, Wiley, 2012.
9. J. Wegener, C. R. Keese and I. Giaever, *Exp Cell Res*, 2000, **259**, 158-166.
10. C. Xiao and J. H. Luong, *Biotechnol Prog*, 2003, **19**, 1000-1005.
11. J. H. Yeon and J. K. Park, *Anal Biochem*, 2005, **341**, 308-315.
12. J. Wegener, S. Zink, P. Rösen and H. Galla, *Pflugers Arch*, 1999, **437**, 925-934.
13. S. Cho, E. Gorjup and H. Thielecke, *Ann Anat*, 2009, **191**, 145-152.
14. C. Hildebrandt, H. Büth, S. Cho, Impidjati and H. Thielecke, *J Biotechnol*, 2010.
15. S. J. Galli, M. Tsai and A. M. Piliponsky, *Nature*, 2008, **454**, 445-454.
16. K. Benson, S. Cramer and H.-J. Galla, *Fluids Barriers CNS*, 2013, **10**, 1-11.
17. R. Meissner, B. Eker, H. Kasi, A. Bertsch and P. Renaud, *Lab Chip*, 2011, **11**, 2352-2361.
18. J. Gottschamel, L. Richter, A. Mak, C. Jungreuthmayer, G. Birnbaumer, M. Milnera, H. Breuckl and P. Ertl, *Anal Chem*, 2009, **81**, 8503-8512.
19. L. Richter, C. Stepper, A. Mak, A. Reinthaler, R. Heer, M. Kast, H. Brueckl and P. Ertl, *Lab Chip*, 2007, **7**, 1723-1731.
20. G. M. Birnbaumer, P. A. Lieberzeit, L. Richter, R. Schirhagl, M. Milnera, F. L. Dickert, A. Bailey and P. Ertl, *Lab Chip*, 2009, **9**, 3549-3556.
21. C. Jungreuthmayer, G. Birnbaumer, P. Ertl and J. Zanghellini, *Sens Actuat*, 2012, **162**, 418-424.
22. C. Jungreuthmayer, G. M. Birnbaumer, J. Zanghellini and P. Ertl, *Lab Chip*, 2011, **11**, 1318-1325.
23. J. Steinkuehler, V. Charwat, L. Richter and P. Ertl, *J Phys Chem. B*, 2012, **116**, 10461-10469.
24. L. Richter, V. Charwat, C. Jungreuthmayer, F. Bellutti, H. Brueckl and P. Ertl, *Lab Chip*, 2011, **11**, 2551-2560.
25. C. M. Hwang, Y. Park, J. Y. Park, K. Lee, K. Sun, A. Khademhosseini and S. H. Lee, *Biomed Microdev*, 2009, **11**, 739-746.
26. S. Shang, F. Yang, X. Cheng, X. F. Walboomers and J. a. Jansen, *Euro Cell Mat*, 2010, **19**, 180-192.
27. B. Lindholm-Sethson, P. Geladi, R. E. Koeppe, O. Jonsson, D. Nilsson and A. Nelson, *Langmuir*, 2007, **23**, 5029-5032.
28. B. Lindholm-Sethson, J. Nystrom, M. Malmsten, L. Ringstad, A. Nelson and P. Geladi, *Anal Bioanal Chem*, 2010, **398**, 2341-2349.
29. J. E. Phelps and N. DePaola, *Am. j. physiol, Heart circ. physiol.*, 2000, **278**, H469-H476.
30. N. DePaola, J. E. Phelps, L. Florez, C. R. Keese, F. L. Minnear, I. Giaever and P. Vincent, *Ann Biomed Eng*, 2001, **29**, 648-656.

31. Y. Shikata, A. Rios, K. Kawkitinarong, N. DePaola, J. G. Garcia and K. G. Birukov, *Exp. Cell. Res.*, 2005, **304**, 40-49.
32. Y. Fang, *Int. J. Electrochem.*, 2011, **2011**.
33. Y.-C. Toh, T. C. Lim, D. Tai, G. Xiao, D. van Noort and H. Yu, *Lab Chip*, 2009, **9**, 2026-2035.
34. Y.-C. Toh, C. Zhang, J. Zhang, Y. M. Khong, S. Chang, V. D. Samper, D. van Noort, D. W. Hutmacher and H. Yu, *Lab Chip*, 2007, **7**, 302-309.
35. C. A. Goubko and X. Cao, *Mater Sci Eng C*, 2009, **29**, 1855-1868.
36. H. Ma, T. Liu, J. Qin and B. Lin, *Electrophoresis*, 2010, **31**, 1599-1605.
37. S. Chung, R. Sudo, P. J. Mack, C. R. Wan, V. Vickerman and R. D. Kamm, *Lab Chip*, 2009, **9**, 269-275.
38. S. K. Sia and G. M. Whitesides, *Electrophoresis*, 2003, **24**, 3563-3576.
39. A. S. Attia, K. A. Schroeder, E. H. Seeley, K. J. Wilson, N. D. Hammer, D. C. Colvin, M. L. Manier, J. J. Nicklay, K. L. Rose and J. C. Gore, *Cell Host Microbe*, 2012, **11**, 664-673.
40. F. H. Epstein, E. H. Choy and G. S. Panayi, *New Eng J Med*, 2001, **344**, 907-916.
41. N. J. Zvaifler, *Adv Immunol*, 1973, **16**, 265-336.
42. A. Mantovani, P. Allavena, A. Sica and F. Balkwill, *Nature*, 2008, **454**, 436-444.
43. N. T. Ashley, Z. M. Weil and R. J. Nelson, *An Rev Ecol Evol Syst*, 2012, **43**, 385-406.
44. B. H. Mevik and R. Wehrens, *J Stat Software*, 2007, **18**.
45. H. Martens, *Chemomet Intell Lab*, 2001, **58**, 85-95.
46. A. Rohman, D. L. Setyaningrum and S. Riyanto, *Int J Spec*, 2014, **2014**.
47. R. D. Cramer, D. E. Patterson and J. D. Bunce, *J Am Chem Soc*, 1988, **110**, 5959-5967.
48. D. V. Nguyen and D. M. Rocke, *Bioinform*, 2002, **18**, 39-50.
49. A.-L. Boulesteix and K. Strimmer, *Brief Bioinform*, 2007, **8**, 32-44.
50. T. Mehmood, H. Martens, S. Sæbø, J. Warringer and L. Snipen, *Algorithm Mol Biol*, 2011, **6**, 27.
51. S. Hou, Q. Sun and D. Xia, *Natural Computation*, 2010, **6**.
52. A. R. McIntosh and N. J. Lobaugh, *Neuroimage*, 2004, **23**, S250-S263.
53. V. Charwat, M. Purtscher, S. F. Tedde, O. Hayden and P. Ertl, *Lab Chip*, 2013, **13**, 785-797.
54. N. H. Cole, *Current Protocols in Cell Biology*, 2001, 1. B. 1-1. B. 26.
55. S. Kassis and P. H. Fishman, *J Biol Chem*, 1982, **257**, 5312-5318.
56. M. F. Ethier, M. Medeiros, F. D. Romano and J. G. Dobson, *Exp Gerontol*, 1992, **27**, 287-300.
57. D. Lindner, C. Zietsch, P. M. Becher, K. Schulze, H.-P. Schultheiss, C. Tschöpe and D. Westermann, *Biochem Res Int*, 2012, **2012**.
58. M. T. Goldberg, Y.-P. Han, C. Yan, M. C. Shaw and W. L. Garner, *J Invest Dermatol*, 2007, **127**, 2645-2655.
59. J. Uchida, K. Kanai, K. Asano, S. Watanabe, T. Hisamitsu and H. Suzaki, *In Vivo*, 2004, **18**, 767-770.
60. M. Chemel, B. Le Goff, R. Brion, C. Cozic, M. Berreur, J. Amiaud, G. Bougras, S. Touchais, F. Blanchard and M. Heymann, *Ann. Rheum Dis.*, 2012, **71**, 150-154.
61. B. Kloesch, T. Becker, E. Dietersdorfer, H. Kiener and G. Steiner, *Int Immunopharmacol.*, 2013, **15**, 400-405.
62. T. Lederer, S. Clara, B. Jakoby and W. Hilbert, *Microsyst. Technol.*, 2012, **18**, 1163-1180.
63. D. Holmes, D. Pettigrew, C. H. Reccius, J. D. Gwyer, C. van Berkel, J. Holloway, D. E. Davies and H. Morgan, *Lab Chip*, 2009, **9**, 2881-2889.

64. D. Malleo, J. T. Nevill, L. P. Lee and H. Morgan, *Microfluid Nanofluid*, 2010, **9**, 191-198.

High-frequency impedance spectroscopy combined with time resolved biomarker quantification and multivariate data analysis enables sensitive monitoring of cell population dynamics.